Alekseyev V.A. Factors affecting the rate of formation of acid drainage water in the dumps of rocks containing sulfides

Vernadsky Institute of Geochemistry and Analytical Chemistry RAS, Moscow (alekseyev-v@geokhi.ru)

Abstract. This current environmental problem is primarily related to the oxidation of pyrite, the most common sulfide. Pyrite oxidation accelerates with increasing temperature, pH, Fe^{3+} and O_2 concentrations in the solution, in the presence of iron-oxidizing bacteria, and temperature and pressure gradients. It slows down in the presence of some ligands and other sulfides (galvanic effect), with an increase in grain size and water content in pores. The rate of the overall reaction is controlled not by the oxidation of Fe^{2+} in solution or the diffusion of O_2 in the surface layer, but by the reactions on the surface and the rate of delivery of O_2 into the dump. Modeling of dump weathering is not yet able to accurately predict the composition of draining water due to the simplification of calculations and models, but it has proved effective in assessing the impact of various parameters on the rate of the process. To improve the models, it is important to use reliable rate equations for both pyrite and other minerals that neutralize solutions.

Keywords: *acidic rock drainage, pyrite oxidation rate, influencing factors*

Weathering of rock dumps containing sulfides (primarily the most common pyrite) can lead to the formation of acidic rock drainage (ARD) with a high metals content, which creates a serious environmental problem. The aim of this work is to critically analyze experimental and computational data evaluating the efficiency and accuracy of measuring individual parameters that affect the rate (r) of pyrite oxidation. This is important for building adequate predictive models.

In the presence of oxygen and water, pyrite (FeS_2) is oxidized by reactions (Chandra, Gerson, 2010):

$$FeS_2 + 3.5O_2 + H_2O \rightarrow Fe^{2+} + 2SO_4^{2-} + 2H^+, \quad (1)$$

$$Fe^{2+} + 0.25O_2 + H^+ \rightarrow Fe^{3+} + 0.5H_2O, \quad (2)$$

$$FeS_2 + 14Fe^{3+} + 8H_2O \rightarrow 15Fe^{2+} + 2SO_4^{2-} + 16H^+, \quad (3)$$

$$Fe^{3+} + 3H_2O = Fe(OH)_3 + 3H^+ . \quad (4)$$

Here, the oxidant is not only O_2, but also Fe^{3+}. The reactions (1) and (3) run in parallel with the rates determined at 25°C by the equations (Williamson, Rimstidt, 1994):

$$r_1 = 10^{-8.19} m_{DO}^{.05} m_{H^+}^{-0.11}, \text{ at pH 3-10} \quad (5)$$

$$r_3 = 10^{-6.07} m_{Fe^{3+}}^{0.93} m_{Fe^{2+}}^{-0.4}, \text{ at pH 0.5- 3} \quad (6)$$

where r is the rate of pyrite oxidation (mol m^{-2} s^{-1}), m is the molality (mol/kg) of the dissolved components indicated by subscripts (*DO* is dissolved oxygen). The total rate of pyrite oxidation can be represented by the sum of equations (5) and (6). At pH < 3, the main contribution to the total rate is given by equation (6), and at pH > 3 by equation (5) (Fig. 1a).

The reaction (2) in acidic solutions proceeds very slowly (Fig. 1b, line 2). Therefore, reaction (2) is considered to control the rate of the subsequent reaction (3), for which it supplies the oxidant Fe^{3+} (Singer, Stumm, 1970). This is true only for sterile conditions but in natural conditions at pH 1.5-3.5, the reaction (2) is accelerated by iron-oxidizing bacteria by 6 orders of magnitude (Fig. 1b, dashed line), while the reaction (3) is accelerated only by an order of magnitude (Fig. 1c).

The differences in the oxidation rates of different pyrite samples with different isomorphic admixtures reach one order of magnitude (Williamson, Rimstidt, 1994). The seffect of temperature on r is estimated at 2 orders of magnitude, if we take into account the real values of the temperature range (0-70°C) and activation energy (56 kJ/mol). Phosphate and oxalate have a strong deterrent effect (Fig. 1d). In a mixture with other sulfides, pyrite acts as a cathode and dissolves more slowly, while other sulfides act as an anode and dissolve faster (galvanic effect) (Fig. 1e).

The value of r increases with an increase in the proportion of air in the pores, but it decreases with time (Fig. 1f). The latter is usually explained by the deposition of a layer of solid reaction products on the surface of the pyrite grains, which prevent the free access of O_2 to the fresh surface of the pyrite. This process is described by the contracting spherical core hypothesis with the coefficient of oxygen diffusion through the crust of the reaction products.

Another, perhaps more plausible explanation is related to the dissolution of active ultrafine particles and surface defects that were formed during the grinding of the mineral and disappeared as a result of dissolution. Such a mechanism is typical, for example, for rock-forming minerals (Gautier et al., 2001), which, over a long time, dissolve at a constant rate normalized to the geometric surface area of the initial grains. For pyrite, the duration of the experiments usually did not exceed 100 days (Fig. 1f), which was not enough to reach the plateau with a constant oxidation rate. In longer experiments, the rate of pyrite oxidation decreased in the first 100 days, but then it remained approximately at the same level, although its fluctuations were quite significant (Fig. 1g).

The pH of the solutions after draining the dumps is determined by the ratio of the contents of minerals that produce and consume acid, as well as the weathering rates of these minerals. Near-neutral drainage solutions are more favorable, since the dissolving heavy metals are sorbed by Fe(III) hydroxide or co-precipitated together with it. To predict the composition of drainage water, static and kinetic tests are usually used, which, however, have a number of disadvantages. Static tests do not take into account the kinetics of mineral dissolution, and kinetic tests are limited in time and distort the results

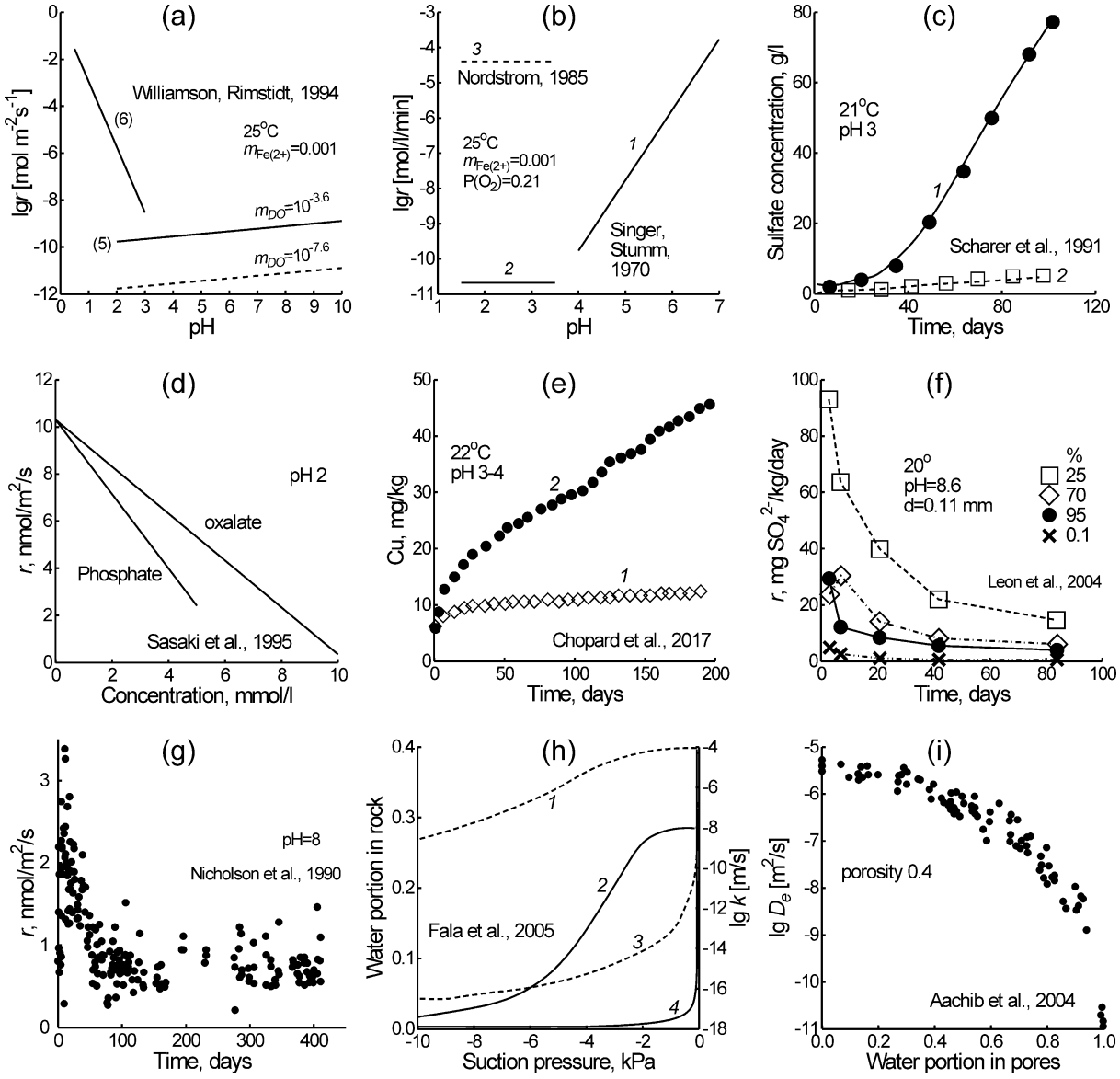

Fig. 1. Dependencies that affect the formation of acidic rock drainage:
(a) *r vs* pH for reactions of pyrite oxidation (equations (5) and (6)). The magnitude of the $m_{Fe(III)}$ was determined by the solubility of $Fe(OH)_3$.
(b) *r vs* pH for the reaction (2) in the absence of bacteria (*1*, *2*) and in their presence (*3*).
(c) Concentration of SO_4^{2-} *vs* time during the oxidation of pyrite in the presence of bacteria (*1*) and in their absence (*2*).
(d) Pyrite *r vs* the concentration of phosphate or oxalate.
(e) ΣCu in solution *vs* time during dissolution of pure chalcopyrite (*1*) and its mixture with pyrite (*2*).
(f) *r vs* time at different water content in the pores of crushed pyrite.
(g) *r vs* time in the presence of water and air in the pores of crushed pyrite.
(h) Water fraction (*2, 4*) and hydraulic conductivity *k* (*1, 3*) for sand (*1, 2*) and gravel (*3, 4*) *vs* suction pressure.
(i) Oxygen diffusion coefficient in the pores (D_e) *vs* water fraction in pores.

due to different conditions in the dumps and in the laboratory humid cells.

More promising may be mathematical modeling of the weathering process of rock dumps using known laws of physics and chemistry with parameters measured experimentally or directly in the dumps for specific cases. The advantage of this method is the ability to calculate the evolution of the process for large time intervals (tens of years) both in the past (checking the conformity of the model to a natural object) and in the future (predicting the behavior of the ARD).

To describe the filtration of water in porous dumps, the Richards equation is usually used (Bouchemella et al., 2015). The hydraulic properties of the porous medium in this equation (water retention curve and hydraulic conductivity) are described using empirical models with coefficients determined experimentally for specific rocks (Fig. 1h) The limitation is due to the fact that these functions depend on many parameters that are difficult to account for by calculation. These are the pore size distribution, pore surface composition and structure, and pore shape. The use of different empirical models to describe the hydraulic properties of a porous medium can lead in some cases to significantly different simulation results.

The oxygen required for the oxidation of pyrite is supplied inside the dump mainly by the diffusion of O_2 molecules through the air or water medium that fills the pores. For pores with variable water and air content, the effective diffusion coefficient D_e is calculated. For this purpose, various diffusion models are used with fitting parameters determined experimentally for specific rocks. With an increase in the proportion of water in the pores from 0 to 1, the value of D_e decreases by 5 orders of magnitude (Fig. 1i), which corresponds to a proportional decrease in the rate of pyrite oxidation.

In ARD modeling, instead of the pyrite oxidation rate equation, the reaction (2) rate equation of Fe^{2+} oxidation in solution is sometimes used (Gerke et al., 1998), mistaking reaction (2) as the stage controlling the rate of the entire reaction. Sometimes the pyrite oxidation rate equation is not considered at all, only the reaction stoichiometry is taken into account. In this case, the control stage of the entire process is considered to be the slow transport of O_2 to the surface of pyrite grains (Molson et al., 2005). However, the depletion of O_2 at pyrite should lead to a slowdown in its oxidation (dashed line in Fig. 1a), i.e., in modeling, you need to consider both. Unfortunately, the dissolution kinetics of rock-forming minerals is almost not used in the ARD modeling, although there is a lot of such data. Their use would allow us to evaluate the effectiveness of ARD neutralization for specific cases, i.e., to approach the models closer to natural objects.

The size of the pieces in the dumps varies from <0.1 microns to >1m, but in the models all the pieces are conventionally considered as spheres of equal size (equivalent diameter) and with the same surface area as for the actual mixture of particles of different sizes (Aubertin et al., 1998). These spheres evolve within the framework of the shrinking sphere hypothesis (Chandra, Gerson, 2010; Molson et al., 2005) with additional coefficient of oxygen diffusion through the crust of secondary minerals on the surface of the spheres. This coefficient is usually used as a fitting parameter of models (Gerke et al., 1998; Molson et al., 2005; Wilson et al., 2018), and its value varies greatly (10^{-11}-10^{-15} m^2/s), which raises doubts about its reliability. The hypothesis is also poorly suited for dumps in the geometric sense, since small grains of sulfides are usually located inside larger pieces of the host rock (Ghorbani et al., 2011).

Air transport inside the dump is a more efficient mechanism for oxygen delivery to the pyrite than diffusion. It occurs in larger pores under the influence of a pressure gradient (wind, a decrease in air volume when O_2 is consumed) or temperature gradient (at heat release during pyrite oxidation) (Lefebvre et al., 2001).

Modeling has shown its effectiveness in identifying additional factors that accelerate or slow down the formation of ARD. In particular, the effectiveness of using a fine-grained coating as a capillary barrier that slows down the access of O_2 into the dump was confirmed (Molson et al., 2005). In ARD modeling, there are a large number of equations and parameters with their own errors, which are summed up and can lead to incorrect solutions. Therefore, an important task of modeling remains the refinement of the equations used and the parameters measured in an independent way.

ARD prevention is primarily associated with the coating of dumps with materials that are poorly permeable to O_2 and water (cement, bitumen, clay, sewage sludge, tailings without sulfides, silt, ash, sludge, slag). If the neutralizing potential of the rock is low, alkaline materials are added to the dump: lime, limestone, dolomite, gypsum, ash, slag, cement dust, phosphates, sugar foam, bauxite (Park et al., 2019; Skousen et al., 2019). To suppress the activity of bacteria, bactericides are used: anionic surfactants, cleaning agents, organic acids, food preservatives. Experiments have shown that many organic substances (sodium oleate, humic acid, phospholipids, diethylenetriamine (DETA), triethylenetriamine (TETA), etc.) form a passivating layer on the surface of pyrite, which prevents its dissolution (Park et al., 2019). The coating of sulfide grains with a protective shell (microencapsulation) of Fe(III) phosphate, silica, organosilane, Ti-, Si-, and Al-catechol is promising.

ARD remediation includes methods of acid neutralization, aeration, precipitation of metal hydroxides, and sulfate reduction of metals in bioreactors. Methods are also proposed to extract useful components from the ARD and purify the water for reuse (Naidu et al., 2019). These are direct and reverse osmosis, nanofiltration, membrane distillation, dialysis, ion exchange, etc. Recycling of sulfide-containing waste into a structural or geopolymer material is possible (Park et al., 2019).

References

Aachib M., Mbonimpa M., Aubertin M. Measurement and prediction of the oxygen diffusion coefficient in unsaturated media, with applications to soil covers // Water, Air, Soil Pollut. 2004. Vol. 156. P. 163-193.

Aubertin M., Ricard J.-F., Chapuis R.P. A predictive model for the water retention curve: application to tailings from hard-rock mines // Can. Geotech. J. 1998. Vol. 35. P. 55-69.

Bouchemella S., Seridi A., Alimi-Ichola I. Numerical simulation of water flow in unsaturated soils: Comparative study of different forms of Richards's equation // Eur. J. Env. Civil Eng. 2015. Vol. 19. P. 1-26.

Chandra A.P., Gerson A.R. The mechanisms of pyrite oxidation and leaching: A fundamental perspective // Surf. Sci. Rep. 2010. Vol. 65. No 9. P. 293-315.

Chopard A., Plante B., Benzaazoua M., Bouzahzah H., Marion P. Geochemical investigation of the galvanic effects during oxidation of pyrite and base-metals sulfides // Chemosphere. 2017. Vol. 166. P. 281-291.

Fala O., Molson J., Aubertin M., Bussière B. Numerical modelling of flow and capillary barrier effects in unsaturated waste rock piles // Mine Water Environ. 2005. Vol. 24. No 4. P. 172-185.

Gautier J.-M., Oelkers E.H., Schott J. Are quartz dissolution rates proportional to B.E.T. surface areas? // Geochim. Cosmochim. Acta. 2001. Vol. 65. No 7. P. 1059–1070.

Gerke H.H., Molson J.W., Frind, E.O. Modelling the effect of chemical heterogeneity on acidification and solute leaching in overburden mine spoils // J. Hydrol. 1998. Vol. 209. P. 166-185.

Ghorbani Y., Becker M., Mainza A., Franzidis J.-P., Petersen J. Large particle effects in chemical/biochemical heap leach processes – A review // Miner. Eng. 2011. Vol. 24. P. 1172-1184.

Lefebvre R., Hockley D., Smolensky J., Lamontagne A. Multiphase transfer processes in waste rock piles producing acid mine drainage: 2. Applications of numerical simulation // J. Contam. Hydrol. 2001. Vol. 52. No 3-4. P. 165-186.

León E.A., Rate A.W., Hinz C., Campbell G.D. Weathering of sulphide minerals at circum-neutral-pH in semi-arid/arid environments: Influence of water content // Proc. 3rd Australian New Zealand Soils Conf. 5-9 Dec. 2004 (ed. B. Singh). Vol. 1. 2004. University of Sydney. P. 1-7.

Molson J.W., Fala O., Aubertin M., Bussiere B. Numerical simulations of pyrite oxidation and acid mine drainage in unsaturated waste rock piles // J. Contam. Hydrol. 2005. Vol. 78. No 4. P. 343-371.

Naidu G., Ryu S., Thiruvenkatachari R., Choi Y., Jeong S., Vigneswaran S. A critical review on remediation, reuse, and resource recovery from acid mine drainage // Environ. Pollut. 2019. Vol. 247. P. 1110-1124.

Nicholson R.V., Gillham R.W., Reardon E.J. Pyrite oxidation in carbonate-buffered solution: 2. Rate control by oxide coatings // Geochim. Cosmochim. Acta. 1990. Vol. 54. No 2. P. 395-402.

Nordstrom D.K. The rate of ferrous iron oxidation in a stream receiving acid mine effluent // In: Selected Papers in the Hydrologic Sciences (ed. S. Subitzky). U.S. Geological Survey Water Supply Paper 2270. Washington: DC, 1985. P. 113-119.

Park I., Tabelin C.B., Jeon S., Li X., Seno K., Ito M., Hiroyoshi N. A review of recent strategies for acid mine drainage prevention and mine tailings recycling // Chemosphere. 2019. Vol. 219. P. 588-606.

Sasaki K., Tsunekawa M., Hasebe K., Konno H. Effect of anionic ligands on the reactivity of pyrite with Fe(III) ions in acid solutions // Colloids Surf. A. 1995. Vol. 101. No 1. P. 39-49.

Scharer J. M., Garga V., Smith R., Halbert B. E. Use of steady state models for assessing acid generation in pyritic mine tailings // Proc. 2nd Int. Conf. on the Abatement of Acidic Drainage. V. 2. Montreal: CANMET, 1991. P. 211-230.

Singer P.C., Stumm W. Acid mine drainage – the rate limiting step // Science. 1970. Vol. 167. No 3921. P. 1121-1123.

Skousen J.G., Ziemkiewicz P.F., McDonald L.M. (2019) Acid mine drainage formation, control and treatment: Approaches and strategies // Extr. Indust. Society. 2019. Vol. 6. No 1. P. 241-249.

Williamson M. A., Rimstidt J. D. The kinetics and electrochemical rate-determining step of aqueous pyrite oxidation // Geochim. Cosmochim. Acta. 1994. Vol. 58. No 24. P. 5443-5454.

Wilson D., Amos R.T., Blowes D.W., Langman J.B., Ptacek C.J., Smith L., Sego D.C. Diavik Waste Rock Project: A conceptual model for temperature and sulfide content dependent geochemical evolution of waste rock – Laboratory scale // Appl. Geochem. 2018. Vol. 89. P. 160-172.

Grishantseva E.S., Alekhin Yu.V. Experimental study of migration mobility of microelements in bottom sediments of Ivankovo reservoir UDC 550.4.02

Department of Geology, M.V. Lomonosov Moscow State University, Moscow (shes99@mail.ru)

Abstract. Here we describe the results of a study on the relative migration mobility of trace elements in bottom sediments and a silty fraction from bottom sediments of the Ivankovo Reservoir at the conditions of inflow of contaminated surface waters. Examination of the sorption properties of bottom sediments of the Ivankovo Reservoir which is a source of drinking water for the city of Moscow is of great ecological and practical importance and would help to evaluate the possibility of secondary contamination

of surface waters. To study the migration mobility of trace elements in laboratory conditions, we carried out a series of dynamic experiments, when bottom sediments in an undisturbed composition and a silty fraction isolated from bottom sediments were employed as chromatographic adsorption-deposition columns through which the adjacent surface waters of both natural composition and contaminated with microelements were filtered. This allowed us to plot the adsorption-desorption curves and obtain the series of mobility of a large number of trace elements from bottom sediments and the silty fraction of bottom sediments.

Keywords: *migration mobility of trace elements; bottom sediments.*

1 INTRODUCTION The aim of this work was to study the relative migration mobility of trace elements and adsorption-desorption processes during the interaction of contaminated surface waters and bottom sediments. Examination of the sorption properties of bottom sediments is of great practical importance and would help to evaluate the possibility of secondary contamination of surface waters. To study the processes occurring during the interaction of contaminated natural waters with bottom sediments and suspended matter, we carried out a series of dynamic filtration experiments. The methodological approach and experimental techniques in these experiments were similar to those that are used for chromatographic separation on columns with the processing of the results by the method of input concentration curves described in the works of Alekhin et al. (2013)

2 MATERIALS AND METHODS The object of the study was the bottom sediments from the Melkovo site of the Ivankovo Reservoir. The Ivankovo Reservoir located in the Tver Region is one of the main sources of drinking water for the city of Moscow; therefore, the protection of its ecological state is an important strategic objective. The sampling of bottom sediments was carried out in June 2017 from the upper 0-10 cm layer using the GOIN tube. The bottom sediments of the Melkovo site are represented by lightweight fine sandy loam.

To study the relative mobility of trace elements and obtain the series of the migration mobility of elements under dynamic conditions, we carried out an experiment with two columns: 1) a column filled with bottom sediments in an undisturbed composition; 2) a column filled with a dusty-silty fraction isolated from bottom sediments. The separation of a fine size fraction (<1 μm) from bottom sediments was carried out by the method of standard sedimentation analysis. Through the columns, aqueous solutions of various composition were sequentially filtered: 1) natural water adjacent to bottom sediments (Melkovo site) that was filtered through a membrane filter with a pore diameter of 0.2 μm; 2) filtrate of natural waters (Melkovo site) contaminated with increased (up to 2-2.5 orders of magnitude), but equal concentrations of a large selection of trace elements, followed by analysis of the series of mobility by the method of output concentration curves.

In experiment 1, in the first filtration unit on top of inert filter substrates, we formed a membrane from bottom sediments in an undisturbed composition, while in the second unit – from a dusty-silty fraction isolated from the bottom sediments of the Melkovo site. Through these units, we passed natural water sampled in the same site and preliminarily filtered through a Vladipor MFAS-OS-1 filter with a pore diameter of 0.2 μm. In experiment 2, in two filtration units on top of inert filter substrates, we formed membranes from bottom sediments and from the dusty-silty fraction of bottom sediments of the Melkovo site. Through these units, we passed natural water filtered through a filter with a pore diameter of 0.2 μm and contaminated with a polyelement standard ICP-MS-68B Solution A (High-Purity Standards). The standard containing 48 elements (Al, As, Ba, Be, Bi, B, Cd, Ce, Cs, Cr, Co, Cu, Dy, Er, Eu, Gd, Ga, Ho, In, Fe, La, Pb, Li, Lu, Mn, Nd, Ni, Pr, Rb, Sm, Sc, Se, Sr, Tb, Tm, U, V, Yb, Y, Zn) was diluted in such a way that the initial concentrations of all elements in the solution were the same and comprised 75±5 μg/L. Both experiments were carried out with the same initial materials of the columns (bottom sediments, silty fraction of bottom sediments), but with different filtrant solutions, until steady-state pH values were reached in the output filtrate. Sampling of filtrate was carried out after 50, 100, 150, 200, 250 ml of filtrant passed through the columns throughout the entire experiment (2 weeks). The volumetric rate of the downward filtration was kept constant at 1 ml/h, the mass of material in the column was 5 g. The filtration rate and the volume of material placed in the columns were chosen taking into account the dispersity of the samples to ensure comparable scales of convective and diffusion transfer of elements during chromatographic separation. In sequentially collected filtrates and in solutions supplied to membranes with material (bottom sediments, silt fraction), we carried out potentiometric measurements (pH) and determined the content of elements by inductively coupled plasma mass spectrometry (ICP-MS).

3 RESULTS During the experiment, the following characteristics were determined: $C_{initial\ solution}$, μg/L – the concentration of the element in the supplied initial solution; C_{sample}, μg/L – the concentration of the element in the filtrate; ΔC, μg/L – the change in the concentration of the element in the filtrate after the interaction of the solution with bottom sediments and suspended matter at a specific moment of observation ($\Delta C = C_{sample} - C_{initial\ solution}$). To characterize the processes of adsorption-desorption of elements by bottom sediments and

suspended matter from the initial solutions, we calculated the local values of the interaction coefficients (R) upon reaching the steady state by the values of the potentiometric indicators. The calculation results are provided in Table 1. For a wide range of elements, the adsorption-desorption curves were plotted (Fig. 1). The R<0 values indicate the predominance of the processes of adsorption of elements by bottom sediments and suspended matter; the R>0 values indicate the predominance of desorption processes. To calculate them, we normalized ΔC (μg/L) in the filtrates for the content of each element in the corresponding bottom sediments or the silty fraction of bottom sediments ($C_{bottom\ sediments}$, μg/kg), taking into account the mass of the material (bottom sediments, suspended matter) (m, kg) on the membrane and the volume of the filtered solution (V_{sample}, L): $R = \Delta C \cdot V_{sample}/C_{bottom\ sediments} \cdot m$.

As expected, in the course of the experiment the initial adsorption accumulation was followed by the desorption of each microelement as a result of ion exchange for such macroelements of natural waters as Ca, Mg, Na. In this case, the limiting steady state is not reached, and to characterize the adsorption-desorption processes, it is necessary to compare the integral values of the delay of the adsorption-desorption process (Alekhin et al., 2013). Moreover, the values of the integral coefficient of interaction during the processes of ion exchange consistently change with time, while preserving the series of mobility. Therefore, for the experiment with the filtration of natural water contaminated with a large number of elements, we calculated the values of the integral interaction coefficient using the formula $R_\Sigma = 1 - (\Sigma(C_{sample} \cdot V_{sample})/(C_{initial\ solution} \cdot V_{sample}))$, where C_{sample} is the concentration of the element in the filtrate, μg/L; $C_{initial\ solution}$ is the concentration of the element in the supplied initial solution, μg/L; V_{sample} is the volume of the sampled filtrate, L.

Table 1. Values of interaction coefficients

dusty-silty fraction of bottom sediments		bottom sediments	
Be	0.0659	Sr	0.0107
U	0.0104	U	0.0095
Zn	0.0082	V	0.0031
Mn	0.0063	Ni	0.0019
Sr	0.0056	Zn	0.0009
V	0.0055	Ag	0.0007
Ni	0.0034	Cr	0.0004
Ag	0.0010	Eu	0.0003
Ba	0.0008	Zr	0.0002
Li	0.0006	Mn	0.0001
Cr	0.0005	Ti	0.00002
Rb	0.0003	Nd	-0.00002
Zr	0.0003	Ce	-0.00004
Eu	0.0002	La	-0.00004
La	0.00003	Ba	-0.00009
Ce	-0.00001	Rb	-0.0002
Ti	-0.00001	Li	-0.0004
Nd	-0.00003	Pb	-0.0031
Pb	-0.0006	Cu	-0.0105
Cu	-0.0107		

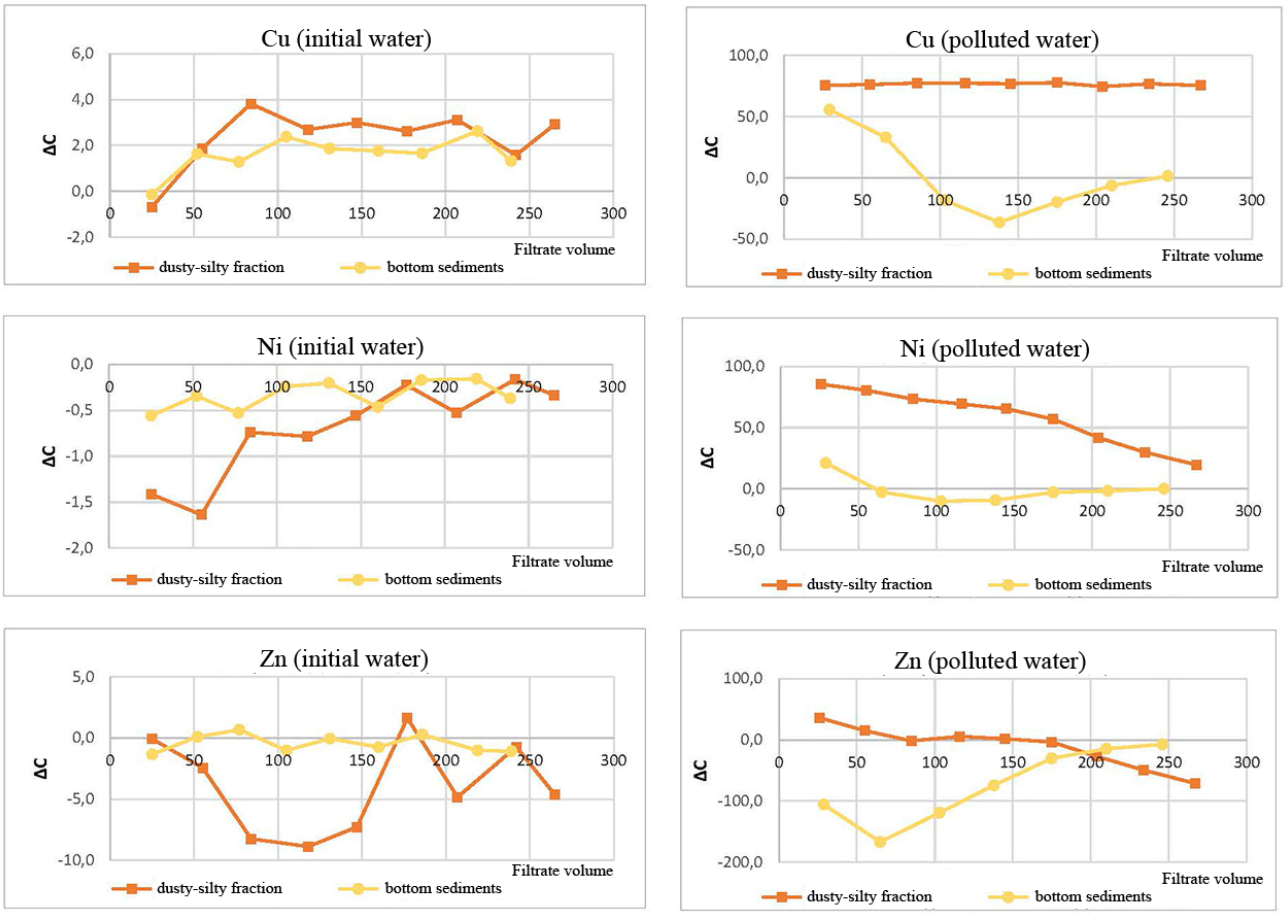

Fig.1. Adsorption-desorption curves for Cu, Ni, Zn.

CONCLUSION The obtained results show that the sequences of elements in the series of mobility for natural water filtered through bottom sediments and silt fraction are similar to each other. When filtering contaminated natural water, the calculated values of the integral interaction coefficients show that the elements are more actively sorbed by the silt fraction. The highest values of the interaction coefficients were obtained for Be, U, Zn, Sr, Mn, V, Ni. In this case, the series of migratory mobility for bottom sediments and silt fraction were very different. For a number of elements, the adsorption process was rather quickly followed by desorption. As to rare earth elements, lightweight elements were found to bind more strongly. The study of the migration mobility of elements under dynamic conditions, when a thin-layer membrane comprised of bottom sediments and suspended matter is considered as a separate adsorption-precipitation chromatographic column, makes it possible to quantitatively assess migration of the elements based on interaction coefficients as extraction and delay coefficients and to obtain the series of migration mobility of the elements during interaction of surface waters with bottom sediments and suspended matter.

The authors thank Makarova M. A. for advice on setting up the experiment and Bychkova Ya. V. for help in performing the ICP analysis.

The work was supported by the RFBR grant № 19-05-00519.

References

Alekhin Yu. V., Drozdova O. Yu., Zavgorodnyaya Yu. A., Motuzova G. V. Migration of elements in the podzolic soil of the Vladimir Meschera: laboratory experiment// Vestn. Mosk.un-ta Ser.4. Geology. 2013. No. 6. p. 53-60.

Kotelnikov A.R.[1], Akhmedzhanova G.M.[1], Suk N.I.[1], Kotelnikova Z.A.[2], Belousova E.O.[1], Martynov K.V.[1], Ananiev V.V.[3] Study of carbon-containing rocks of Zaonezhya

UDC 550.4.02, 553.9

[1]IEM RAS, Chernogolovka Moscow district, (kotelnik@iem.ac.ru); [2]IGEM RAS, Moscow; [3]IVS RAS, Petropavlosk-Kamchatskii

Abstract. Geochemical treatment of the composition of the carbon-bearing rocks of Zaonezhie was carried out. It is shown that the geochemical spectra of biophilic elements (V, Ni, Cu, Zn, As, Mo, Ag, Cd, U) show a high convergence of their compositions with the compositions of coal. The study of the mineral composition of carbon-bearing rocks has been carried out. Thermobarogeochemical methods were used to study fluid inclusions in quartz veins. The maximum value of TP-parameters of metamorphism was recorded using a calcite-dolomite thermometer and a phengite barometer (T=400°C; P=5 ± 1 kbar), and the formation of muscovites and chlorites correspond to the

late stages of the process: T = 300-150°C; P = 3.3-1 kbar. The study of leaching of elements from carbon-containing rocks at T=25, 90 and 200°C was carried out experimentally. The influence of temperature and composition of solutions on the process of hydrolytic leaching is shown.

Keywords: *carbon-bearing rocks, fluid inclusions, leaching, lithophilic, chalcophilic, biophilic elements*

To assess the conditions for the genesis and evolution of carbon-bearing rocks (CBR) in Zaonezhie (South Karelia), a study of shungites from the Maksovsky and Zazhoginsky quarries was carried out.

Basically, the study was carried out by the method of X-ray spectral microanalysis, as well as by the method of X-ray fluorescence analysis, some of the elements were analyzed in parallel on an atomic absorption spectrometer "Quant". For this, the silicate part of the sample was transferred into solution by acid decomposition.

ANALYSIS OF THE SUBSTANCE OF CARBON-CONTAINING ROCKS Analysis of the purely carbonaceous matter of carbon-bearing rocks (shungites) from the Maksovsky quarry showed the following average composition (in wt%): C – 79.89(4.15); O – 5.50(2.34); Na – 0.11(0.23); K – 0.18 (0.27); S – 0.30(0.05); Cl – 0.11(0.20); Sum – 86.08. No silicate substance was found. The dominance of potassium over sodium in the salt load and small amounts of sulfur and chlorine can be noted. The variation in carbon content is insignificant (V_x = 5.2%). Analysis of the composition of shungite, carried out by Sadovnichy (2016), showed a rather high content of X-ray amorphous substance – up to 53 wt%. The samples we studied from the Zazhogino and Maksovo quarries contained up to 40 wt% carbonaceous matter. We also performed partial analyzes of the silicate substance of CBR for the content of trace and impurity elements (V, Cr, Co, Ni, Cu, Zn, Rb, Sr, Y, Ba, Nb, Mo, Pb, Th, U) by X-ray fluorescence and atomic absorption analyzes. Paired correlation coefficients were calculated for these data, taking into account a confidence level of 95%. It was assumed that the distribution of elements in the CBR corresponds to the normal one.

It is possible to estimate the origin of the studied CBR using the method of correlation of the spectra of trace and trace elements with various rocks and minerals of organogenic origin. Such objects for comparison were selected: 1) black shales (Yudovich, Ketris, 1994); 2) oil from various regions of Russia (Kalinin, 2009); 3) coal (Yudovich, Ketris 2002; Ketris, Yudovich, 2009; Arbuzov et al., 2019); 4) asphaltites (Marakushev, 2009). It was shown that, according to the geochemical spectra of biophilic elements (V, Ni, Cu, Zn, As, Mo, Ag, Cd, U), there is a high convergence of the compositions of CBR with the compositions of black shale (Fig.1a) and coals (Fig.1b). It is obvious that the high correlation with black shales for all trace elements is due to the proportion of lithophilic elements of volcanogenic-sedimentary origin in carbon-bearing rocks, while the proportion of biophilic elements brings the composition of CBR closer to coal.

MINERALS OF CARBON-CONTAINING ROCKS The study of the mineral composition of carbon-bearing rocks has been carried out. The following minerals has been found.

Group of sulfide minerals: pyrite, pyrrhotite, chalcopyrite, sphalerite, pentlandite, lead sulfoselenide, arsenic-containing pyrite.

Phosphates: apatite, monazite.

Oxides: mainly quartz, often containing carbonaceous matter and sulfide minerals. According to the classification of Sadovnichy (2016) this is a typical collomorphic quartz, genetically related to the bio- and chemogenic conditions of the formation of protomaxovite matter. There are also quartz veins.

Carbonates: magnesium-containing calcite and dolomite with FeO content up to 1.6 wt.% were found in the metamorphosed carbonate-silicate rocks surrounding the CBR massifs.

Silicates: titanite is quite widespread in the rocks of the Maksovo quarry. Secondary minerals include kaolinite.

Aluminosilicates. An extensive group of minerals, represented by structural types (1) frame minerals (feldspar group); (2) layered silicates (mica group – biotite, phengite, paragonite); (3) diorthosilicates – allanite (structurally similar to epidote). A rather rare mineral, pumpelliite, is also sometimes found. The studied samples contain individual grains of epidote and chlorite.

STUDY OF FLUID INCLUSIONS To study fluid inclusions (FI), quartz-bearing samples were taken from carbon-bearing rocks of the Tolvuya village area. These were samples from the Maksovsky quarry (vein quartz) and the Tolvuya-Tetyugino site (silicified lidite). Microthermometric studies of FI in quartz were carried out in all samples. It is shown that these inclusions are represented by the types L and G + L.

The average salinity of the solution is 11.62 (% NaCl-eq) with an root mean square error (S_x) of 2.8 (for n=6). The average density of the fluid, determined from the homogenization temperatures, is 0.95 g/cm^3 (n = 10; S_x = 0.01). The compositions of mineral-forming solutions from silicified lidites – 11.62 (% NaCl-eq) – are practically the same as for the quartz veins of the Maksovsky quarry – 9.85 (% NaCl-eq). The presence of syngenetic types of inclusions G + L and L indirectly indicates their formation from a layered fluid.

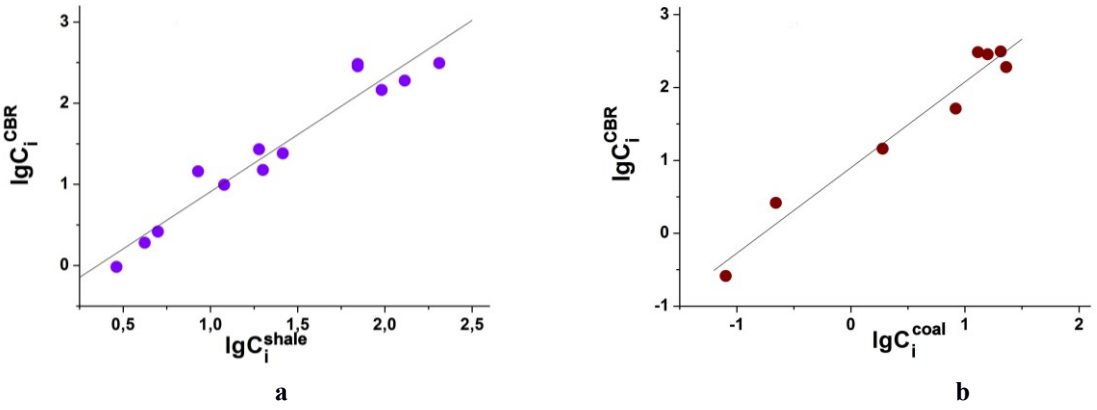

Fig. 1. Correlation of the concentration of trace and impurity elements of carbon-bearing rocks (CBR) and black shale (shale) (a), coals (coal) (b) on biophilic elements.

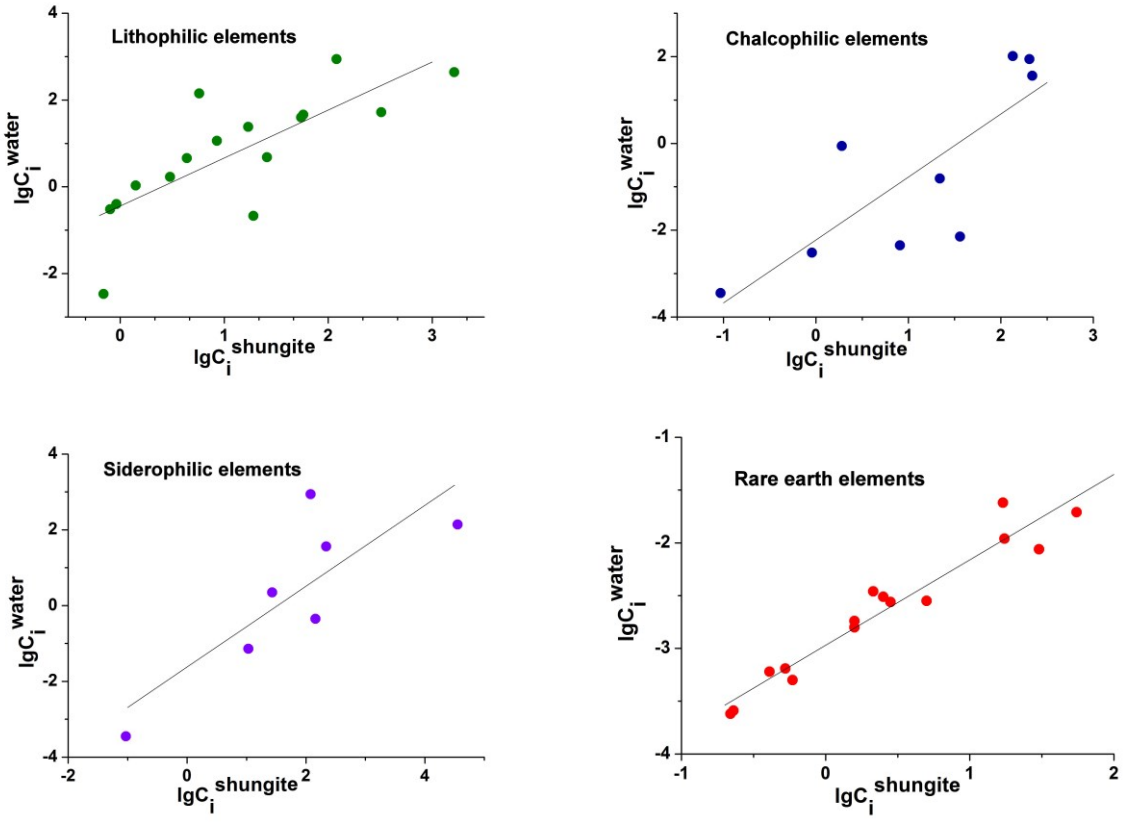

Fig. 2. Correlation of the composition of surface waters (water) with the content of elements in carbonaceous rocks (shungite).

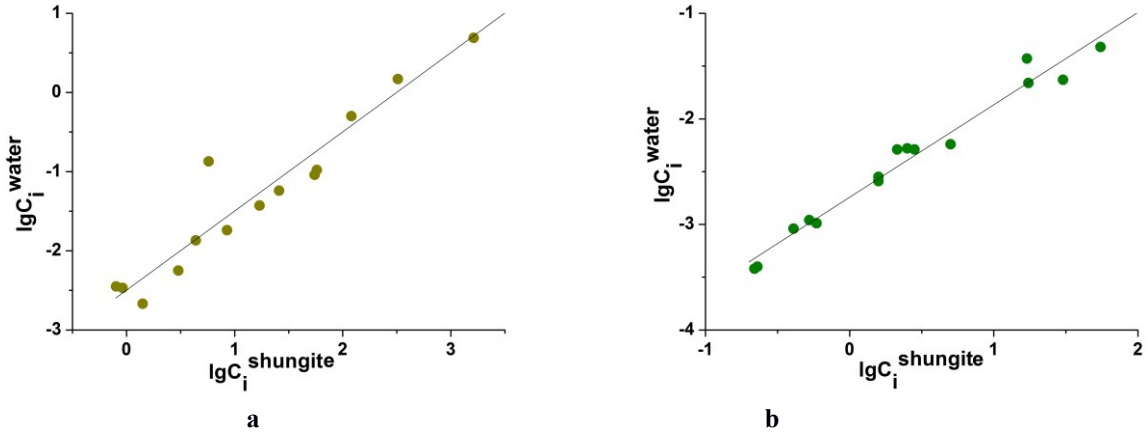

Fig. 3. Correlation of the compositions of solutions (water) with the content of elements in carbon-containing rocks (shungite) in leaching experiments: a – for lithophilic, b – for rare earth elements.

MINERAL THERMOMETRY AND BAROMETRY For the purposes of mineral thermometry, samples of the carbonate-silicate rocks containing CBR (Tolvuya-Tetyugino area) and samples of carbon-bearing rocks, in which the necessary parageneses were found, were selected.

Estimation of the temperatures of mineral formation according to the compositions of muscovites (in the presence of paragonite) (Yoder, Eugster, 1955; Popov, 1969) gives the following range of values: 200-410°C. Chlorite thermometer calculation (Cathelineau, Nieva, 1985) showed T = 240 ± 10°C.

Calculation of pressure according to the compositions of phengites (Massonne, Schreyer, 1987) for temperatures of 400°C gives the following range of values: 3.5 – 6.8; average 5.5 ± 1.4 kbar. Another group of phengites, present in the Maksovo CBR, satisfying the criteria: Si (f.e.)> 3.25; ∑(K+Na)> 0.7 and SumVI = 1.86 – 2.27 shows pressure values from 7.6 to 9.8 kbar, average value is 8.2 ± 0.8 kbar.

It is shown that the pressure values obtained by different methods are generally consistent with each other. The pressures estimated from fluid inclusions in quartz are 0.5 – 1 kbar lower than those determined from phengite compositions. Obviously, the peak of metamorphism of maksovites was recorded by calcite-dolomite and muscovite-paragonite thermometers and a phengite barometer (T = 400°C; P = 5.5 ± 1.4 kbar). For 400°C, FI determined pressures from 4.2 to 5.9 kbar (average is 5.0 ± 0.4 kbar), and chlorites and muscovite (X_{Na}^{Ms} = 0.012) recorded the late stages of the process: T = 240-200°C; pressure from 2.3 to 1.5 kbar.

Based on the geochemical analysis of the compositions of CBR it is possible to conclude about their genesis from an organomineral substance, which is a mixture of a "sapropel" organic residue with volcanic-sedimentary matter and a significant amount of silica introduced by deep fluids.

SURFACE WATER COMPOSITIONS The composition of the surface waters of the Zazhogino and Maksovo quarries has been investigated. Correlation of their compositions with the content of elements in carbonaceous rocks for lithophilic, biophilic, chalcophilic, siderophilic and rare earth elements is shown (Fig. 2).

The study of leaching of elements from carbon-containing rocks at T=25, 90 and 200°C was carried out experimentally. The correlation of the compositions of the obtained solutions with the content of elements in carbon-containing rocks has been established (Fig. 3). The influence of temperature and composition of solutions on the process of hydrolytic leaching is shown.

This work was supported by the AAAA-A18-118020590150-6 program.

References

Arbuzov S.I., Vergunov A.V., Ilyenok S.S., Ivanov V.A., Ivanov V.P. „ Soktoev B.R. Geochemistry, mineralogy and genesis of a rare metal-coal deposit in stratum XI in the south of the Kuznetsk basin // Geosphere issledovaniya. 2019. N. 2 P. 35–61.

Cathelineau M, Nieva D. A chlorite solid solution geothermometer The Los Azufres (Mexico) geothermal system // Contrib Mineral Petrol. 1985. V. 91. P. 235-244

Kalinin E.P. Geochemical specificity of oil and its nature // Bulletin of the Institute of Geology of the Komi Scientific Center of the Ural Branch of the Russian Academy of Sciences. 2009. N. 1. P. 6-12.

Marakushev A.A. Geochemistry and genesis of black shale // Bulletin of the Institute of Geology of the Komi Scientific Center of the Ural Branch of the Russian Academy of Sciences. 2009. N. 7. P. 2-4.

Massonne H.J., Schreyer B.W. Phengite geobarometrie based on the limiting assemblage with K–feldspar, phlogopite, and quarz. Contrib. Mineral. Petrol. 1987. Vol. 96, № 2. P. 212-224.

Popov A.A. Potassium and sodium in natural muscovites and paragonites // Proceedings of the A.E. Fersman Mineralogical Museum. 1969, issue 19. P. 61-69.Sadovnichy R.V. Mineral and technological features of shungite rocks of the Maksovsky deposit (Zazhoginsky ore field). Candidate Dissertation of geological and mineralogical sciences. Petrozavodsk. 2016. 137 p.

Yoder H.S., Eugster H.P. Synthetic and natural muscovites.— Geochim. et Cosmochim. Acta, 1955, N 8, p.225-238.

Yudovich Ya.E., Ketris M.P. Trace elements in black shale. Yekaterinburg: UIF "Science". 1994. 304 p.

Yudovich Ya.E., Ketris M.P. Inorganic substance of coals. Yekaterinburg: Ural Branch of the Russian Academy of Sciences. 2002. 423 p.

Kotova N.P. Effect of fluoride concentration and fluid pressure on Nb_2O_5 solubility

Institute of Experimental Mineralogy RAS, Chernogolovka Moscow district (kotova@iem.ac.ru)

Abstract. The influence of fluoride concentration and fluid pressure on niobium oxide solubility in HF solutions with a concentration of 0.1 and 1 m at 550 °C and 50, 100, 200 and 500 MPa is experimentally studied. It is established that in 0.1 and 1.0 m HF solutions Nb content decreases by an order of magnitude with increasing pressure from 50 to 200 MPa. With a further increase in pressure to 500 MPa, the niobium content practically does not change and remains in the range of $10^{-3.5}$ mol/kg H_2O in 0.1m HF solution and $10^{-1.7}$ mol /kg H_2O in 1 m HF solution.

***Keywords**: experiment, oxide niobium, hydrothermal solubility, pressure, fluoride solutions*

The development of scientifically-based criteria for forecasting and searching for deposits of economically important metals requires a clearer understanding of their formation conditions, transfer forms of ore elements and their behavior in various physicochemical environments. Experimental studies of ore minerals solubility under controlled physicochemical parameters are necessary to create reliable experimental databases. These databases are necessary to determine the prevailing transfer forms of ore elements, to estimate their thermodynamic properties and then to construct quantitative models of ore elements fractionation in the natural environment, to determine the conditions for the formation of large deposits and the validity of existing genetic hypotheses of their origin. Research parameters cover T-P-X-f (O_2) conditions corresponding to magmatic and hydrothermal processes of mineral and ore formation. The question of the genetic relationship of magmatism and hydrothermal ore formation for endogenous deposits of ore elements, P - T conditions of ore-bearing solution source, remains debatable. Experimental and thermodynamic studies of ore minerals solubility are a necessary step in these researches. Therefore, the assessment of the limiting concentrations of ore elements in hydrothermal solutions in a wide range of T-P-X parameters required for constructing a quantitative model of the ore formation process is an urgent problem of ore genesis.

New experimental data on the solubility of niobium oxide (β-Nb_2O_5), an analog of the natural mineral nioboxide, were obtained in aqueous fluoride solutions consisting of 0.1 and 1.0 m HF at 550 °C and 50, 100, 200, and 500 MPa. The run duration was 10 - 18 days. Experiments at 550 °C and 50 to 100 MPa were performed on a hydrothermal line. A sealed-capsule quench technique was employed.

Experiments at 550 °C and 200 to 500 MPa were carried out on a high gas pressure installation with internal heating (gas bomb). It allows reaching pressures up to 6 MPa and temperatures up to 1400 °C. Run temperatures were measured with an accuracy of ± 5 °C. The pressure was regulated with a maximum uncertainty of ± 5 MPa. Regulation and maintenance of the required temperature in the working chamber of the furnace is carried out using the TRM-101 OVEN thermostat through two S-type thermocouples (Pt90Rh10-PT100). Thermocouples are mounted at the top and close to the bottom of the chamber to control the temperature gradient. The chamber system pressure is set from above by pure argon gas pressure. The lid of the working chamber is made of pyrophyllite. Aluminum oxide and kaolin wool serve as filler in the chamber with ampoules.

The quenched aqueous solutions were then analyzed using ICP/MS (Inductively Coupled Plasma Mass Spectrometry) and ICP/AES (Atomic Emission Spectroscopy) for Nb, Ta, Mn, and Fe and admixture elements Ti, W, and Sn.

To control congruent or incongruent dissolution of Nb oxide and to determine chemical composition of newly-formed phases (in case of their detection) the initial materials and solid run products were studied by X-ray diffraction, and electron microprobe analysis (Cam Scan MV 2300 (VEGA TS5130MM).

The experimental results are shown in Fig. 1 and 2. Analysis of the data obtained showed that the trends of the dependence of niobium oxide solubility on pressure in 0.1 and 1m HF solutions are identical. In both cases, with an increase in pressure from 50 to 200 MPa, the solubility of niobium oxide decreases by about 1 order of magnitude for a 1m HF solution, and by 1.5 orders of magnitude for a 0.1 m HF solution.

With a further increase in pressure from 200 MPa to 500 MPa, the equilibrium niobium content practically does not change, remaining at the same level ($10^{-3/5}$ mol/kg H_2O for 0.1 m HF solution and $10^{-1.75}$ mol/kg H_2O for 1m HF solution) (Fig.1).

Comparison of experimental results on the niobium oxide solubility in fluoride solutions showed that at T = 550 °C and P = 50, 100, 200 and 500 MPa at low concentrations of fluorides (0.1 m HF), the solubility of Nb_2O_5 is approximately 1-1.3 orders of magnitude lower than at higher concentrations (1m HF).

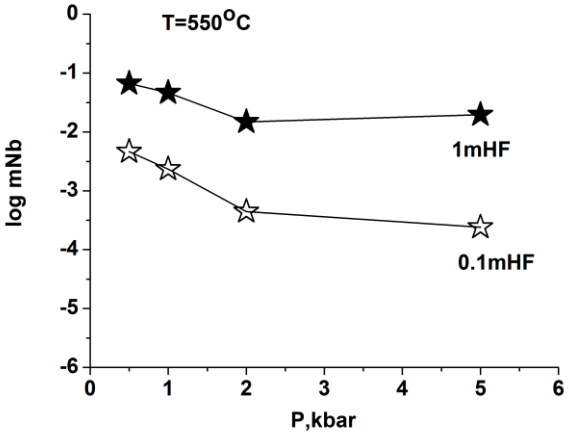

Fig.1. Influence of HF concentration and fluid pressure on the Nb_2O_5 solubility at T = 550 °C (asterisks - 0.1 m HF, shaded asterisks - 1 m HF)

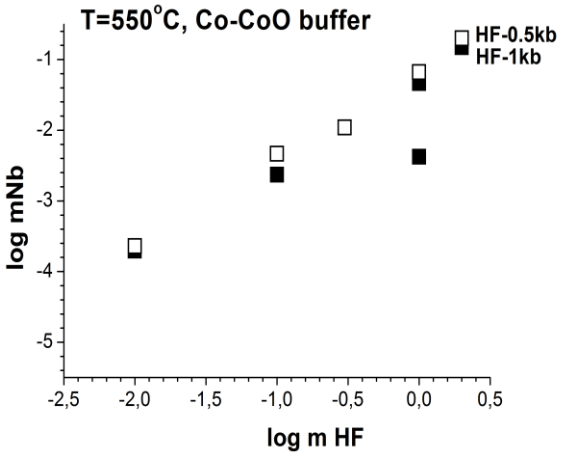

Fig.2. Influence of HF concentration and fluid pressure on the Nb_2O_5 solubility at T = 550 °C (squares-at P = 0.5kb, shaded squares–at P=1kb)

It was experimentally established that a decrease in fluid pressure from 100 to 50 MPa in HF solutions has little effect on the Nb_2O_5 solubility (Fig. 2) (Kotova, 2014). At low concentrations of HF (less than 10^{-2} m), the niobium content in the solution is $10^{-3.5}$ mol/kg H_2O. With an increase in the concentration of fluorine ion, the solubility of Nb_2O_5 strongly increases and at a concentration of HF-1m and higher reaches significant values (10^{-2} – $10^{-1.5}$ mol/kg H_2O), which are quite sufficient for real mass transfer of niobium by hydrothermal solutions (Kotova, 2012).

The studies carried out confirm the earlier conclusion that the solubility of simple oxides (Ta_2O_5 and Nb_2O_5) depends to a greater extent on the concentration of fluoride fluids. P-T conditions have little effect on the solubility of niobium and tantalum.

This work was supported by the grant of RFBR N 20-05-00307

References

Kotova N.P. (2014) Experimental study of Nb_2O_5 solubility in fluoride solutions at 550°C and 500 bar, Experiments in Geosciences, V.20, N1, p. 38-39

Kotova N.P. (2012) Experimental study of concentration dependence of niobium oxide solubility in fluoride solutions at T=550 °C, P = 1000 bar and low oxygen fugacity (Co-CoO buffer) Experiments in Geosciences, V.18, N1, p. 123-125

Tselmovich V.A., Kurazhkovskii A.Yu. Changes in mineral composition of peat thickness under global cooling associated with activations of explosive magmatism UDC 551.590.3

GO Borok IPE RAS., Borok, Yaroslavl dist (tselm@mail.ru)

Abstract. The influence of the activation of explosive volcanism (536 AD) and the subsequent cooling on the ecosystems of peat bogs that formed on the territory of Russia was investigated. The studied peat strata of two bogs had coordinates (55° N, 88° E, and 58° N, 38° E, Kemerovo and Yaroslavl regions). The position of the peat horizons presumably corresponds to the 536 event and was determined by the radiocarbon method. The bottom of these horizons was respectively located at a depth of 120 cm and 105 cm. Micromineralogical studies showed that at these depths peat is enriched in ferro-silicate spherules with a diameter of 0.1-10 microns and is characterized by a relatively high remanent magnetization and density. The thickness of the layer enriched in ferro-silicate spherules and having a relatively high remanent magnetization is on average 7 cm. The thickness of the layer with increased density was 10-20 cm. The probable time interval between the change and restoration of ecosystems was about 200 years.

Keywords: *explosive volcanism, global cooling, peat bogs, microspherules*

Introduction. From historical chronicles it is known that in the area of 536 AD a catastrophic event took place that had a negative impact on the development of both European and, probably, the planetary civilization. The cause of this event has not been definitively established. There is evidence that a significant activation of explosive magmatism took

place in the area of 536 (Larsen et al., 2008; Siebert, Simkin, 2002). At the same time, there is an assumption that the activation of magmatism could coincide or could be triggered by an impact event (Barenbaum, 2013).

Peat strata formed in the Holocene are promising objects, the results of the study of which can be used in the course of argumentation of hypotheses explaining the nature of catastrophic events. In this work, we studied the features of the mineralogical composition of peat horizons that formed after the event of 536. In addition, an attempt was made to assess the impact of this event on changes in biota in the regions in which peat deposits were formed.

Methods and results. We studied cores of peat deposits sampled in regions separated by geographic longitude (Kemerovo and Yaroslavl regions) and remote from places of probable activations of effusive magmatism. The coordinates of the coring points were (55° N, 88° E, and 58° N, 38° E, respectively). The age of the peat horizons was determined by the radiocarbon method. In the studied strata, the rates of peat accumulation differed insignificantly. The peat horizons corresponding to the 536 event were at depths of 120 cm and 105 cm. Measurements of the remanent saturation magnetization (Irs) and density (ρ) of cubic peat samples (with a rib size of 2 cm) showed that near the 120 and 105 cm horizons, peat had a relatively high density ρ and Irs. The density of peat depended both on the amount of mineral matter in its samples and on the state of the biota. The Irs value was determined, first of all, by the amount of mineral matter in the peat samples. Figure 1 shows the dynamics of changes in these parameters in terms of the thickness of the studied peat strata.

Figure 1 shows that the detail of sampling in the studied strata and the detail of determining the dynamics of petromagnetic parameters were somewhat different. Nevertheless, in both strata, a horizon with increased Irs values was recorded. Its thickness was somewhat (7 cm on average). The thickness of the horizon with increased peat density averaged about 15 cm. Magnetometric measurements (Irs) revealed that the peat horizon formed around 536 contained an increased amount of mineral matter (Fig. 1 a, b).

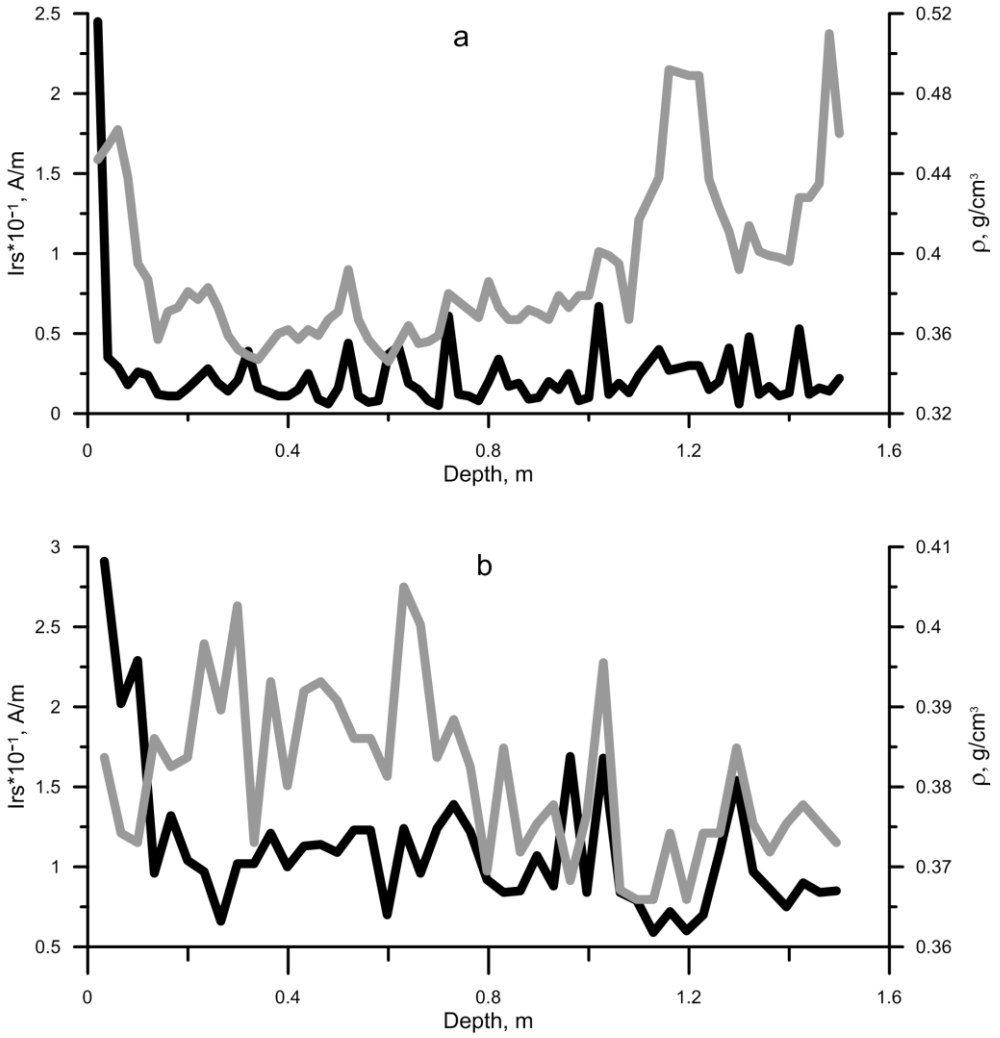

Fig. 1. Variations in Irs (black curve) and ρ (gray curve) by thickness of peat strata in Kemerovo (a) and Yaroslavl (b) regions

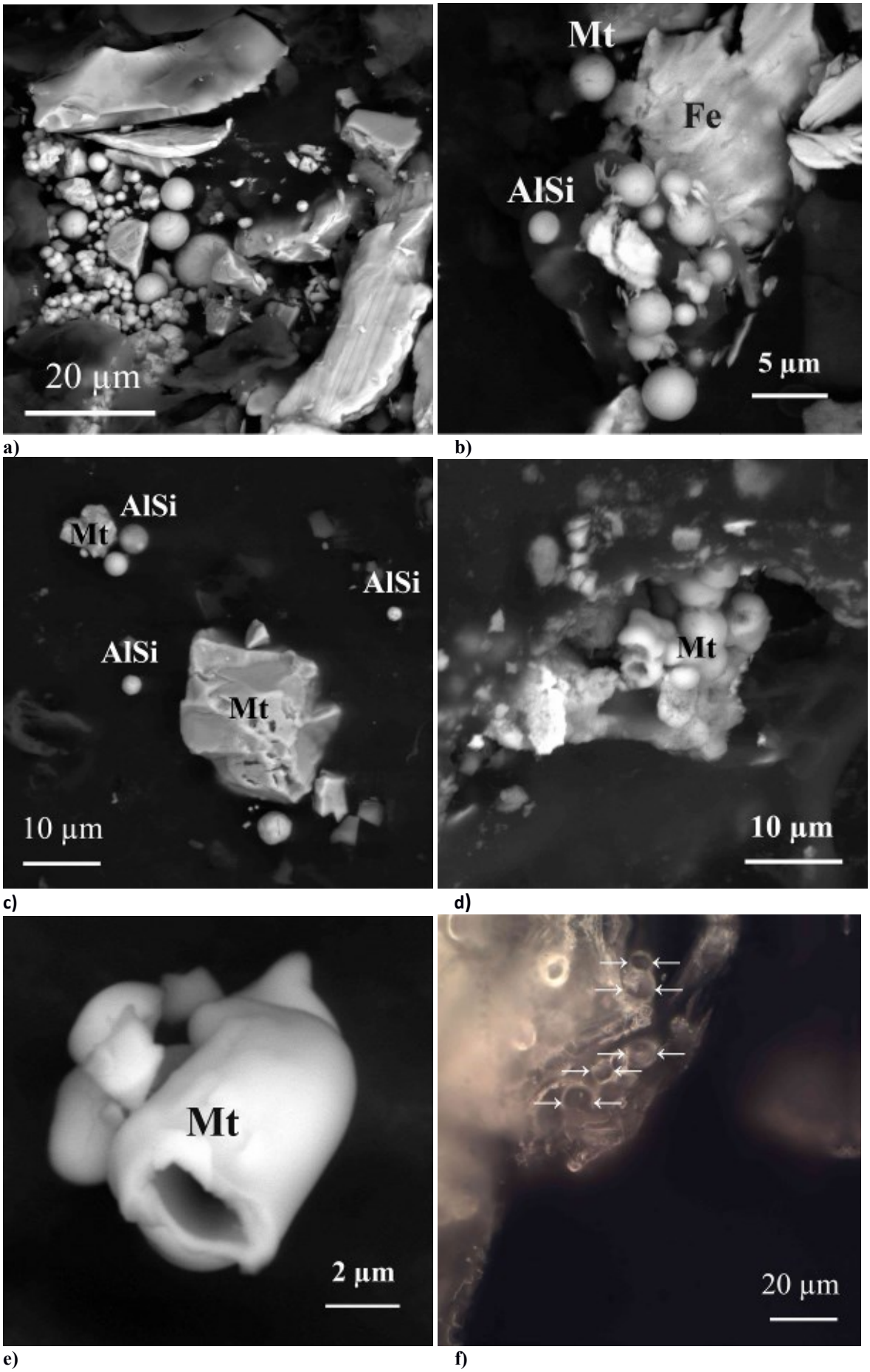

Fig. 2: a) general view of the separated mineral particles, microspheres and native iron, Mt; b) aluminosilicate (AlSi) with an admixture of iron and Mt microspheres and native Fe; c) AlSi microspheres and volcanic Mt; d) a group of small magnetite microspheres; e) individual particles of Mt; f) AlSi microspheres from volcanic ash, North Caucasus volcano.

Microanalysis carried out using the Tescan Vega 2 microanalyzer showed that this horizon (in comparison with other horizons) is enriched in relatively small (10–0.1 μm) ferrosilicate microspheres (Fig. 2 a – f), presumably of volcanic origin. Such particles, in contrast to organic ones, can significantly determine the values of the Irs value. Particles with a predominantly aluminosilicate composition often contain nano-sized precipitates of magnetite and exhibit magnetic properties. Similar particles were isolated by us from volcanic ash (the volcano is located in the North Caucasus, Fig. 2 f, optical microscope). The overlying horizons (10–20 cm) had an increased density. Moreover, the features of their density were not determined by the amount of mineral matter, but were associated with biotic changes.

Conclusions. The study of peat strata made it possible to establish that the event of 536 was accompanied by increased precipitation of ferrosilicate particles and changes in biota. Judging by the thickness of the horizon with increased density, the interval between the change and restoration of the biota was 100–200 years. It can be assumed that effusive magmatism influenced the mineralogical composition of peat horizons at depths of 120 and 105 cm. In this case, small (less than 10 μm) ferrosilicate particles could be transported by air masses. This assumption seems logical, since during the west-east transfer, the relative changes in Irs in the sediments of the Yaroslavl Region were higher than in the sediments of the Kemerovo Region. However, our research does not allow us to completely rule out the cosmogenic cause of the 536 catastrophe.

A possible mechanism for the origin of small aluminosilicate particles may be not only ejection with volcanic ash, but also their additional dispersion by lightning arising in ash clouds (Cherneva et al., 2013). The abundance of aluminosilicate balls that we found in peat may be an indicator of a volcanic eruption of 536 years.

The work was performed on the state order of the IPE RAS

References

Barenbaum A.A. Possible mechanism of heating rocks of the lithosphere by galactic comets // Ural Geological Journal. 2013. No. 1 (91). P. 21-39.

Cherneva N.V., Melnikov A.N., Holzworth R.H, Ivanov A.V., Druzhin G.I., Firstov P.P. Identification of lightning with ash clouds of explosive eruptions in Kamchatka. Solar-terrestrial connections and physics of earthquake precursors. VI International Conference September 9-13, 2013, p. Paratunka, Kamchatka Territory. Collection of abstracts of the VI International conference. Petropavlovsk-Kamchatsky, 2013, pp. 362-367.

Larsen LB, Vinther BM, Briffa KR, Melvin TM, Clausen HB, Jones PD, Siggaard-Andersen M.-L., Hammer CU, Eronen M., Grudd H., Gunnarson BE, Hantemirov RM, Naurzbaev MM, Nicolussi K. New ice core evidence for a volcanic cause of the AD 536 dust veil // Geophys. Res. Letters. 2008. V. 35. L04708. doi: 10.1029 / 2007GL032450.

Siebert L., Simkin T. Volcanoes of the World. 2002. URL: http://www.volcano.si.edu/gvp/world/